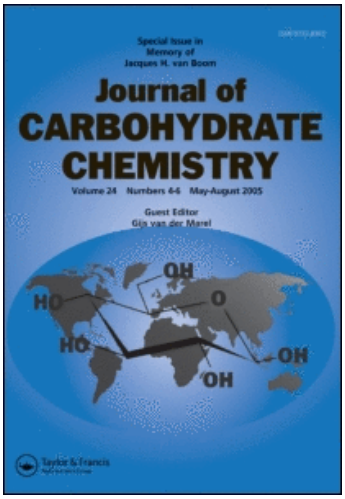

Journal of Carbohydrate Chemistry

Publication details, including instructions for authors and subscription information:
http://www.informaworld.com/smpp/title~content=t713617200

The Conformation of Some Halodeoxy Analogues of Methyl β-Lactoside in D_2O and DMSO-d_6 Solutions

Paloma Fernández[a]; Jesús Jiménez-Barbero[a]
[a] Grupo de Carbohidratos, Instituto de Química Orgánica General, C.S.I.C., Madrid, SPAIN

To cite this Article Fernández, Paloma and Jiménez-Barbero, Jesús(1994) 'The Conformation of Some Halodeoxy Analogues of Methyl β-Lactoside in D_2O and DMSO-d_6 Solutions', Journal of Carbohydrate Chemistry, 13: 2, 207 — 233
To link to this Article: DOI: 10.1080/07328309408009189
URL: http://dx.doi.org/10.1080/07328309408009189

J. CARBOHYDRATE CHEMISTRY, 13(2), 207-233 (1994)

THE CONFORMATION OF SOME HALODEOXY ANALOGUES OF METHYL β-LACTOSIDE IN D_2O AND DMSO-d_6 SOLUTIONS

Paloma Fernández and Jesús Jiménez-Barbero*

Grupo de Carbohidratos, Instituto de Química Orgánica General, C.S.I.C., Juan de la Cierva 3, 28006 Madrid, SPAIN

Received February 8, 1993 - Final Form September 20, 1993

ABSTRACT

The solution conformation of several halodeoxy analogues of methyl β-lactoside **1** has been analysed using molecular mechanics and dynamics calculations and nuclear magnetic resonance data (variable temperature and NOE experiments). The overall shape of all the compounds studied is fairly similar and may be described by conformers included in a low energy region with Φ=-100±40º and Ψ= -135±35º, that is *ca.* 5% of the total potential energy surface calculated for the β(1->4) glycosidic linkages of the disaccharides.

INTRODUCTION

As a part of a project on the molecular recognition between lactose analogues and galactose-binding proteins, we have reported on the binding of methyl β-lactoside[1] (**1**) and all its monodeoxy derivatives by the β-galactoside specific lectins ricin (RCA 60) and

agglutinin (RCA 120), isolated from *Ricinus communis* seeds.[1,2] The observed dissociation constants indicated the involvement of the remote glucose residue having a $^4C_1$ chair conformation in the recognition and binding, mainly through a hydrophobic interaction between the lectins and the C-3 region of the disaccharide, while HO-3', HO-4', and HO-6' of the galactose moiety are involved in hydrogen bonding to the protein. Besides, HO-2' seems to be responsible for a peripheral polar interaction between the disaccharides and the receptors. The total hydrogen bonding donor and acceptor capacity of a hydroxyl group to interact with a polar group may be assessed by using a deoxy analogue.[3] However, knowledge of the role of a given group as a hydrogen bond donor or acceptor has been usually proved through the use of deoxyfluoro[4] or, in general, deoxyhalo compounds. However, care should be taken to draw quantitative conclusions from the variation of association constants observed, since a rearrangement of the local tridimensional structure of the complex may occur due to the higher electronegativity of the fluorine atom with respect to oxygen.[5] An analysis of the recognition phenomenon based on modified substrate analogues must therefore be accompanied by a careful study of the possible changes in their conformation in order to relate structure and activity. On this basis, we now report on the conformation of several deoxyfluoro, deoxyiodo, and deoxybromo analogues of methyl β-lactoside (**1**), namely the methyl 6-deoxy-6-fluoro ß-lactoside (**2**), methyl 6-deoxy-6-iodo ß-lactoside (**3**), methyl 3'-deoxy-3'-fluoro ß-lactoside (**4**), methyl 4'-deoxy-4'-fluoro ß-lactoside (**5**), methyl 4'-deoxy-4'-epi-fluoro ß-lactoside (methyl 4'-deoxy-4'-fluoro ß-cellobioside) (**6**), methyl 6'-deoxy-6'-fluoro ß-lactoside (**7**), and methyl 6'-deoxy-6'-bromo ß-lactoside (**8**) in D_2O and DMSO-d_6 solutions, based on molecular mechanics and dynamics calculations, and nuclear magnetic resonance data, particularly variable temperature experiments, and proton NOE measurements. These compounds have been used as ligands for ricin and agglutinin[6] to disentangle the role of the different hydroxyl groups as hydrogen bond donors or acceptors, and the involvement of the remote glucose residue in the binding, assuming that the conformational changes between the free and bound states will be minor, as reported for the

binding of methyl β-lactoside to ricin-B chain.[7] On the other hand, a recent study on the conformation of methyl melibioside bound to ricin-B has shown[8] that the generally flexible α(1->6) linkage in this α(1->6)-linked disaccharide is held in one of its solution conformations when bound to the protein, and that the glucose moiety is not involved in the binding process. Nevertheless, it has to be observed that the relative orientation of the glucose ring with respect to the galactose residue in the β(1->4) and the α(1->6) linkages is rather different.

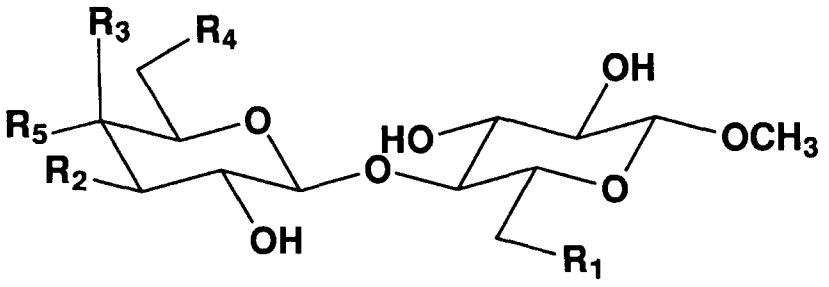

1 R_1-R_4=OH, R_5=H
2 R_1=F, R_2-R_4=OH, R_5=H
3 R_1=I, R_2-R_4=OH, R_5=H
4 R_1=OH, R_2=F, R_3,R_4=OH, R_5=H
5 R_1,R_2=OH, R_3=F, R_4=OH, R_5=H
6 R_1,R_2=OH, R_3=H, R_4=OH, R_5=F
7 R_1-R_3=OH, R_4=F, R_5=H
8 R_1-R_3=OH, R_4=Br, R_5=H

EXPERIMENTAL

Materials.- Compounds **2-8** were prepared in our laboratory and their syntheses will be reported elsewhere.

NMR experiments.- NMR spectra were recorded at 37 °C in D_2O, and at 37 °C and 60 °C in DMSO-d_6 on a Varian Unity 500 spectrometer. Proton chemical shifts were referenced to residual HDO at δ 4.64 ppm or residual DMSO-d_5 at δ 2.49 ppm. Carbon chemical shifts were referenced to external dioxane at δ 67.4 ppm. ^{19}F NMR spectra were recorded at 30 °C on Varian XL-300

spectrometer. Trifluoroacetic acid was used as external standard, and the chemical shifts are given from trichlorofluoromethane.[9]

The double quantum filtered DQF-COSY experiments were performed in the phase sensitive mode using the standard Varian sequence. A data matrix of 256 * 2K points was used to digitize a spectral width of 1500 Hz. 16 scans were used per increment with a relaxation delay of 2 s. The 90º pulse width was 7.5 μs. Prior to Fourier transformation, zero filling was used in F_1 to expand the data to 1K * 2K.

The clean 2D-TOCSY experiments[10] were carried out in the phase sensitive mode using MLEV-17 for isotropic mixing. The mixing time was set to 150 ms. A data matrix of 256 * 1K points was used to digitize a spectral width of 1500 Hz. 16 scans were used per increment with a relaxation delay of 2 s. The 90º pulse width during the mixing period was 22.5 μs. Squared cosine bell functions were applied in both dimensions and zero filling was used to expand the data to 2K * 2K.

The 2D rotating frame NOE (ROESY, CAMELSPIN) experiment were recorded[11] in the phase sensitive mode. The spin-lock period consisted of a train of 30º pulses (2.5 μs), separated by delays of 50 μs. The total mixing time was set to 300 ms. The rf carrier was set at δ 5.5 ppm to minimize spurious Hartmann-Hahn effects.[11,12] A data matrix of 256 * 2K points was used to resolve a spectral width of 3000 Hz. 32 scans were used per increment with a relaxation delay of 2 s. Prior to Fourier transformation, squared sine bell functions shifted by $\pi/3$ were applied in both dimensions and zero filling was used in F_1 to expand the data to 2K * 2K. The pure absorption 2D-NOESY experiments were carried out with mixing times of 300 and 700 ms. A data matrix of 256 * 2K points was used to resolve a spectral width of 1500 Hz. 32 scans were used per increment with a relaxation delay of 2 s. Processing was similar to that reported for ROESY experiments. NOESY and ROESY were integrated using standard Varian software after applying a third order polynomial baseline correction in both dimensions. The total intensity of the added ω_1 cross sections containing diagonal and cross-peaks was given a 100% value.[13] The steady state NOE experiments were performed through the interleaved differential

technique using a saturation delay of 10 s. Between 256 and 512 free induction decays were accumulated for each irradiation site.

The pure absorption one bond proton-carbon correlation experiments were collected in the ^{1}H-detection mode using the HMQC[14] or HSMQC[15] pulse sequences and a reverse probe. A data matrix of 256 • 2K points was used to resolve a spectral width of 8000 Hz and 1500 Hz in F_1 and F_2, respectively. 16 scans were used per increment with a relaxation delay of 2 s and a delay corresponding to a *J* value of 152 Hz. A BIRD-pulse was use to minimize the proton signals bonded to ^{12}C. ^{13}C-decoupling was achieved by the WALTZ scheme. Squared cosine bell functions were applied in both dimensions and zero filling was used in F_1 to expand the data to 2K • 2K.

The pure absorption HSMQC-ROESY experiments were collected in the ^{1}H-detection mode using the pulse sequence 90(^{1}H)-Δ-90(^{1}H,^{13}C) - t_1/2 - 180(^{1}H) - t_1/2 -90(^{1}H,^{13}C)-Δ-SpinLock-Acq(^{1}H) where Δ is 1/2J_{CH} and the Spin Lock time was set to 300 ms. The phase cycling was based on the combination of the original HSMQC[15] and ROESY[11] pulse sequences. A data matrix of 128 * 2K points was used to resolve a spectral width of 8000 Hz and 2500 Hz in F_1 and F_2, respectively. The carrier was set 100 Hz downfield from the most deshielded proton resonance. 256 scans were used per increment with a relaxation delay of 1 s and a Δ delay corresponding to a *J* value of 150 Hz. A BIRD-pulse was use to minimize the proton signals bonded to ^{12}C. ^{13}C-decoupling was not used during acquisition. Squared cosine bell functions were applied in both dimensions and zero filling was used to expand the data to 2K • 4K.

^{13}C NMR spin lattice relaxation times were determined for compounds **2, 3, 5**, and **6** in D_2O at 37º C and in DMSO-d_6 at 37 and 60 °C through the inversion recovery technique using Varian software. Two independent sets of eight delays were used in the determination. The T_1 values were used to estimate the average correlation time (τ_c) of these molecules at the different temperatures assuming isotropic motion and dipole-dipole relaxation only.

Molecular mechanics and dynamics calculations.- The MM2-low energy conformers found previously[1] for **1** (A, B, C/C', D, E) were

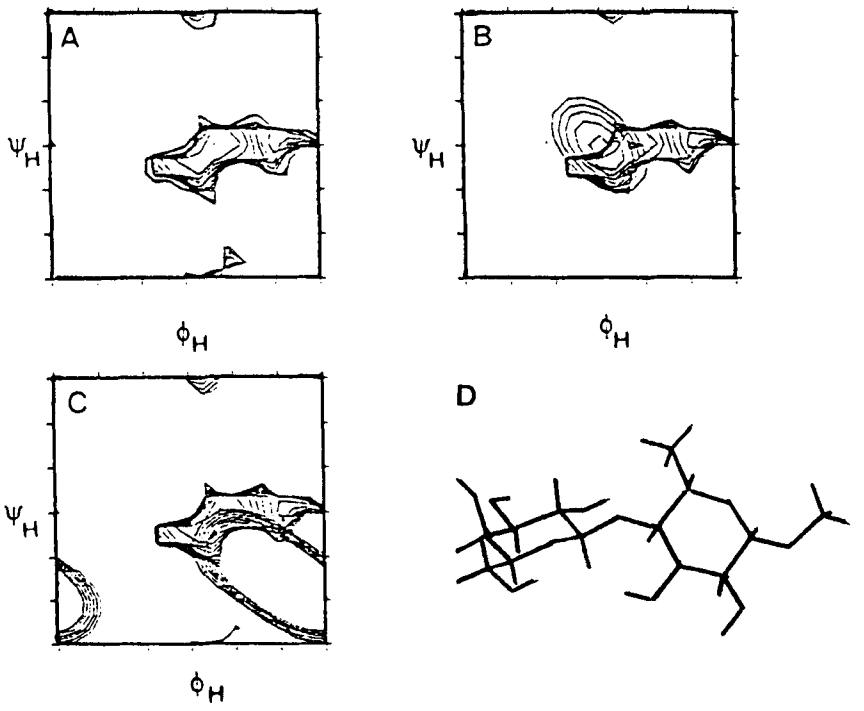

Figure 1.-(A) A Ramachandran-type plot of the isoenergy contours of **2**. (B) Region defined by H-1'-H-4 distances between 2.1 and 2.5 Å. (C) Region defined by O-5'-O-3 distances between 2.7 and 3.2 Å. (D) Starting conformation for the calculation.

modified at the desired position and submitted to further minimization. Glycosidic torsion angles are defined as Φ O-5'-C-1'-O-1'-C-4, Ψ C-1'-O-1'-C-4-C-5, Φ_H H-1'-C-1'-O-1'-C-4, and Ψ_H C-1'-O-1'-C-4-H-4. Only the *gt* conformation of the lateral chain was used for the galactose residue, while both the *gg* and *gt* rotamers were considered for the glucose moiety.[16] In all cases, both Φ and Ψ angles remained close (*ca.* ±5º) to the starting point. A dielectric constant of 1.5 D was used. The geometries of compounds **2**, **3**, **5**, and **6** describing minima A, D, and/or E (*gg* for the glucose residue) were then taken as starting structures for Molecular Dynamics calculations in vacuo by using the CVFF[17] and the Discover 2.8 program.[18] The MD simulations were performed at 303 °K with a dielectric constant of 78 D to simulate the presence of water and a time step of 1 fs. The equilibration time was set to 20 ps while the

total simulation time was 520 ps or 1020 ps. Trajectory frames were saved every 0.5 or 1 ps. The trajectories were then examined with the Analysis module of INSIGHT II.[19] The steady state 1D-NOE and the 2D-NOE experiments were calculated according to the complete relaxation matrix method[20] by using the NOEMOL program[21] for the proton coordinates of conformers A, B, C, and C', and for a Boltzmann distribution of these minima, calculated from the MM2 relative energies at 37 °C. Isotropic motion and no external relaxation was assumed in the calculation process. Since NOEs are extremely dependent on the correlation time, different τ_c values were used in order to get the best match between the experimental and the calculated NOE for a given intraresidue proton pair. 2D-NOESY and 2D-ROESY experiments were used to estimate interproton distances according to the isolated spin pair approximation[22].

RESULTS AND DISCUSSION

Table I shows the values of the estimated populations of the different conformers of **1**, **3-7** obtained by MM2 optimisation of the HSEA minima obtained previously[1] for **1**, along with those obtained by use of the Discover-CVFF programme. Due to the presence of a number of electronegative atoms, these energies should be taken as approximate since they are variable at least 0.5 Kcal/mol.

The predicted distribution of conformers estimated from the relative energy values is also given in Table I. A Ramachandran-type plot of the isoenergy contour of compound **2** is given in Figure 1. The corresponding maps for compounds **3-7** were very similar, as expected for ß(1->4) glycosidic linkages. It can be observed that there are six local minima under a level of relative steric energy of *ca.* 4.00 Kcal/mol, independently of the force-field used, while there is a broad low energy region described by conformers A, B, C, and C' with rather small energy barriers among them.[1] Figure 2 shows stereoscopic views of these low energy conformers for compound **2.** The previously reported X-ray structures for different β(1->4) equatorial linked dissacharides are included in this low energy region.[1] According to the calculations, this low energy region described by Φ=-100±40º, Ψ=-135±35º, and $r_{H\text{-}1'\text{-}H\text{-}4}$=2.4±0.4Å

TABLE I

Estimated Populations (%) for the low energy conformers of **1-3**, **5**, **7**, and **8**, estimated from the MM2[a] and CVFF[b] steric energy values.

Compound	Conformer				
	A	B	C/C'[c]	D	E
	Pop[a]	Pop	Pop	Pop	Pop
1	33.9	37.5	25.6	1.8	0.2
2	34.3	43.7	20.0	1.7	0.3
3	30.0	43.3	24.7	1.7	0.3
5	18.7	70.1	8.7	1.9	0.6
7	25.4	49.2	23.4	1.9	0.6
8	12.5	48.1	37.4	1.7	0.3
	Conformer				
	A	B	C/C'	D	E
	Pop[b]	Pop	Pop	Pop	Pop
1	36.1	31.2	31.0	1.4	0.3
2	40.7	23.3	25.7	5.7	5.6

a. from MM2 energy values. b. from CVFF energy values. c. minimum C shows *gt* orientation for the C-5-C-6 torsion angle of the gluco-pyranose ring, while conformer C' shows *gg* orientation for the C-5-C-6 torsion angle of the glucopyranose ring.

appears to be populated in more than 90% extent while the two minor islands described by conformers D and E are populated less than 5% at 37° or 60°. Nevertheless, the possibility of their existence in solution cannot be discarded *a priori* since the conformation of some interglycosidic acetals synthesized from lactose and cellobiose[23] is that of conformer D, while the recent X-ray analysis of the bound conformation of a biantennary octasaccharide to *Lathyrus Ochrus Isolectin I* has shown the existence of a Man β(1->4) GlcNAc linkage in conformation E, and a Gal β(1->4)GlcNac moiety located in island D.[24,25]

Thus, the stability of the different conformers was studied by using molecular dynamics simulations (MD) with the Discover-CVFF programme. Although the CVFF is a general MD programme not

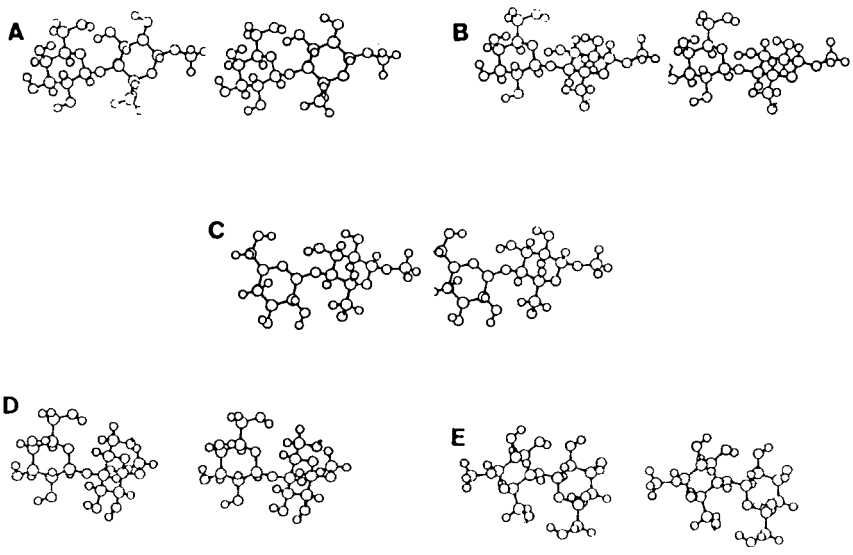

Figure 2.- Stereoscopic views of the low energy conformers of **1**. (A) Φ -70, Ψ -116, (B) Φ -96, Ψ -176, (C) Φ -150, Ψ -156, (D) Φ 60, Ψ -122, (E) Φ -92, Ψ 61.

specifically parametrized for carbohydrates, and therefore does not include any extra potential to account for the anomeric effects,[26] its use in the conformational study of different oligosaccharides has produced satisfactory results.[27] Different conformations of compounds **2**, **3**, **5**, and **6** were used as input geometries for independent 520 ps or 1020 ps simulations at 303 °K. The trajectories of some of them are displayed in Figure 3.

In all cases, no chair to chair or chair to boat interconversions were observed. The average Φ and Ψ angles were calculated to be -80±15º and -135±10º, depending on the starting conformer. It can be observed that the trajectories remained most of the time (>90%) in the broad region described by minima A, B, C, and C'. In fact, only when the calculation started from geometry E, the trajectory spent a fraction of time within this island (*ca.* 200 ps), although the trajectory went again to the low energy region. Also when the starting geometry was that of conformer D, the simulation resulted in a transition to region A-C' within a few picoseconds. Therefore, these results seem to indicate that minima D and E are not stable

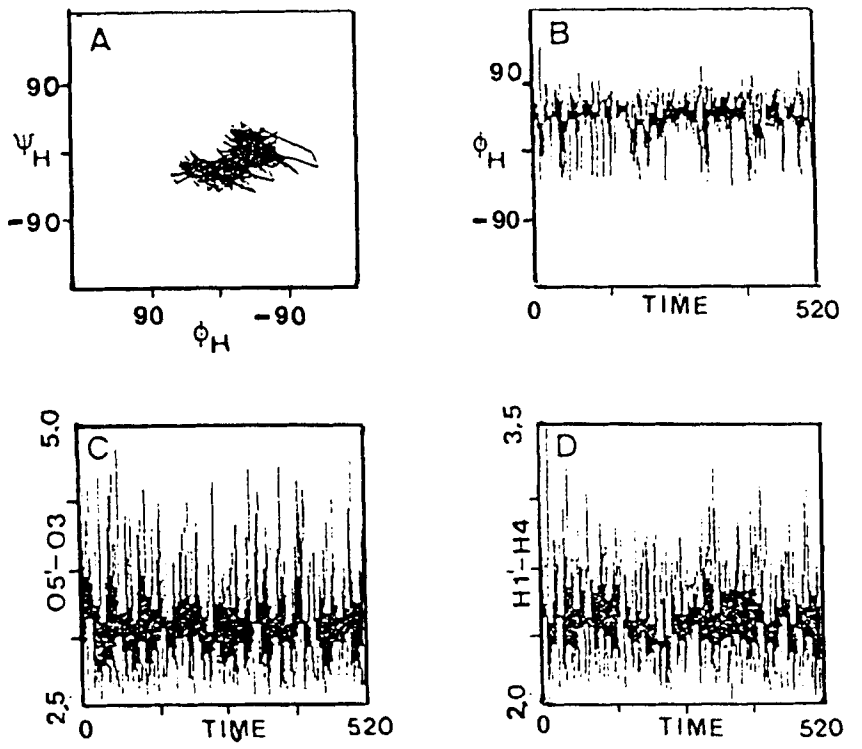

Figure 3.- a. Contour plot of the trajectories (520 ps) calculated from MD simulations for **2**, starting from coordinates corresponding to conformer A. b. History of Φ angle. c. History of O-5'-O-3 distance. d. History of H-1'-H-4 distance.

enough in comparison to conformers A-C', when external factors such as stabilization by hydrogen or covalent bonds or non polar contacts are not involved.[24] In all cases, several transitions between the possible orientations of the C-5-C-6 chains were observed. NMR spectroscopy can be used to distinguish the presence of either conformer.[28,29] All the low energy region described by conformers A, B, C, and C' has short distances between H-4 and H-1', H-3 is close to H-1' in conformer E, H-4 close to H-2' in conformer D, and there is an unique contact between H-1' and $H\text{-}6_{proR}$ or $H\text{-}6_{proS}$ for the *gg* or *gt* rotamers of conformer A, respectively. In addition, conformers A and B can be stabilized by intramolecular hydrogen bond between HO-3 and O-5' since both oxygen atoms are less than 3.0 Å apart. These structural characteristics are shown in

TABLE II
Relevant interatomic distances for the low energy conformers of **1-8**.

Distance(Å)	Conformer(Φ/Ψ)				
	A	B	C/C′	D	E
	Φ(°)				
	-70	-96	-140/-113	60	-92
	Ψ(°)				
	-116	-175	-150/-141	-122	61
H-1'-H-4	2.33	2.34	2.23	>3.5	>3.5
H-1'-H-3	>3.5	>3.5	>3.5	>3.5	1.79
H-1'-H-5	>3.5	>3.5	>3.5	>3.5	2.23
H-1'-H-6_R	2.49[a]	>3.5	>3.5	>3.5	>3.5
H-1'-H-6_S	2.62[b]	>3.5	>3.5	>3.5	>3.5
H-1'-O-3	>3.5	2.48	2.47	>3.5	>3.5
H-1'-X-6	2.52	>3.5	>3.5	>3.5	>3.5
H-2'-H-4	>3.5	>3.5	>3.5	1.94	>3.5
O-2'-O-3	>3.5	>3.5	>3.5	2.93	>3.5
O-5'-O-3	3.02	2.63	3.06	>3.5	>3.5
O-2'-H-6_R	2.96[a]	>3.5	3.12	>3.5	>3.5
O-2'-H-6_S	2.99[b]	>3.5	3.06	>3.5	>3.5

a. *gg* or b. *gt* rotamers around the C-5-C-6 bond.

Table II. The observation of one or two interresidue NOEs and some specific shieldings or deshieldings can impose constraints in the potential energy map as to assess the existence of a given conformation.[30] The previous step for the analysis of the NOE data was the assignment of the different resonances through a combination of homo and hetero 2D-NMR techniques allowed to assign the spectra of compounds **2-8**. Particularly useful were the ^{1}H-detected HMQC and HSMQC experiments to resolve the cases of overlapping signals. The doubling of signals due to the coupling to fluorine was also an important help in the assignment process. The first-order chemical shifts and relevant coupling constants for compounds **1-8** are shown in Tables III-VII.

No important chemical shift differences were detected between **1** and compounds **2-8** in D_2O or DMSO-d_6 solutions, apart from those expected for specific halogen modification. The ^{19}F NMR parameters also agree (Table V) with previously reported data,[9] the

TABLE III

^1H and ^{13}C NMR chemical shifts (δ, ppm) for compounds **1-8** in D_2O solution at 37 °C.

Proton	Compound							
	1	**2**	**3**	**4**	**5**	**6**	**7**	**8**
Glucose residue								
H-1	4.40	4.46	4.47	4.39	4.39	4.37	4.38	4.39
H-2	3.30	3.34	3.32	3.30	3.29	3.28	3.28	3.31
H-3	3.64	3.68	3.68	3.64	3.65	3.63	3.63	3.66
H-4	3.63	3.76	3.59	3.66	3.64	3.62	3.62	3.63
H-5	3.59	3.77	3.41	3.61	3.59	3.57	3.60	3.64
$H\text{-}6_S$	3.98	4.86	3.73	3.98	3.99	3.97	3.98	3.99
$H\text{-}6_R$	3.80	4.79	3.49	3.79	3.80	3.79	3.77	3.80
Galactose residue								
H-1'	4.44	4.46	4.56	4.49	4.53	4.53	4.45	4.47
H-2'	3.53	3.57	3.54	3.83	3.58	3.34	3.54	3.52
H-3'	3.65	3.66	3.67	4.59	3.77	3.82	3.66	3.65
H-4'	3.92	3.95	3.93	4.21	4.84	4.32	3.98	4.03
H-5'	3.72	3.73	3.73	3.72	3.85	3.71	3.97	3.93
$H\text{-}6'_R$	3.78	3.80	3.78	3.78	3.82	3.89	4.62	3.61
$H\text{-}6'_S$	3.75	3.77	3.75	3.73	3.80	3.68	4.60	3.57
Glucose residue								
C-1	104.3	104.5	104.3	104.4	104.2	104.5	104.5	104.4
C-2	74.1	74.0	74.1	74.2	74.3	74.2	74.2	74.1
C-3	75.8	75.5	75.2	74.7	75.7	75.6	76.0	75.6
C-4	79.9	79.5	76.7	79.5	79.7	79.5	79.8	80.6
C-5	76.1	75.9	76.4	75.7	76.2	76.0	76.1	76.1
C-6	61.4	82.5	7.5	61.3	61.4	61.2	61.5	61.6
Galactose residue								
C-1'	104.4	104.2	104.3	103.4	104.4	103.8	104.5	104.4
C-2'	72.3	72.2	72.2	71.0	72.3	74.3	72.1	72.0
C-3'	73.9	73.8	73.8	93.1	72.7	74.8	73.7	73.7
C-4'	69.9	69.8	69.8	68.0	90.8	90.4	69.4	70.4
C-5'	76.7	76.6	76.7	75.3	75.2	74.5	74.9	76.4
C-6'	62.3	62.2	62.3	62.0	61.4	61.3	84.3	31.5

equatorial fluorine atom at position 4' (**6**) appearing deshielded with respect to the axial one (**5**). The chemical shifts of the fluorine atoms at C-6 (**2**) and C-6' (**7**) are very similar, while the fluorine atom of **4** is the most deshielded one. The ^1H NMR chemical shifts for the hydroxylic protons in DMSO at 30 °C and the differences between these values and those determined at 70 °C are given in Table VI. These differences are smaller for HO-3 than for any other

TABLE IV

^1H and ^{13}C NMR chemical shifts (δ, ppm) for compounds **1-7** in DMSO-d_6 solution at 37 °C.

Proton	Compound						
	1	**2**	**3**	**4**	**5**	**6**	**7**
Glucose residue							
H-1	4.09	4.17	4.18	4.10	4.09	4.09	4.09
H-2	3.00	3.03	3.03	3.00	3.00	3.02	3.01
H-3	3.32	3.34	3.35	3.31	3.31	3.33	3.30
H-4	3.29	3.28	3.14	3.30	3.33	3.32	3.31
H-5	3.28	3.55	3.26	3.38	3.28	3.28	3.32
$H\text{-}6_S$	3.74	4.71	3.77	3.73	3.78	3.74	3.74
$H\text{-}6_R$	3.60	4.65	3.39	3.58	3.61	3.62	3.62
Galactose residue							
H-1'	4.19	4.15	4.21	4.26	4.34	4.38	4.30
H-2'	3.31	3.33	3.31	3.58	3.24	3.07	3.35
H-3'	3.30	3.32	3.31	4.35	3.47	3.48	3.36
H-4'	3.61	3.61	3.61	3.89	4.58	4.14	3.65
H-5'	3.45	3.45	3.44	3.43	3.60	3.25	3.83
$H\text{-}6'_R$	3.51	3.52	3.52	3.49	3.49	3.61	4.56
$H\text{-}6'_S$	3.46	3.47	3.46	3.45	3.46	3.50	4.45
O-CH3[a]	3.38	3.37	3.40	3.38	3.39	3.39	3.38
Glucose residue							
C-1	106.1	105.9	105.5	105.2	105.6	105.5	105.9
C-2	75.1	75.0	74.8	75.1	75.3	75.1	75.0
C-3	76.7	76.1	76.1	76.8	76.8	76.8	76.7
C-4	82.5	81.1	86.5	82.4	82.3	82.0	82.3
C-5	76.8	74.9	75.1	76.8	76.8	76.8	76.7
C-6	62.3	84.0	10.6	62.2	62.3	62.2	62.3
Galactose residue							
C-1'	105.7	106.2	105.3	105.3	105.6	104.8	105.4
C-2'	72.4	72.2	72.3	70.8	72.8	75.1	72.3
C-3'	75.0	75.2	75.1	95.6	73.5	75.5	74.8
C-4'	70.0	69.6	70.0	67.9	89.6	91.5	69.9
C-5'	77.4	77.6	77.4	75.9	75.5	75.8	75.3
C-6'	62.4	62.5	62.2	61.8	61.1	62.0	85.3

hydroxyl group in this set of compounds. Moreover, the $J_{HO\text{-}3,H\text{-}3}$ values were always <1.5 Hz, indicating a average dihedral angle close to 90º, while the remaining of the vicinal couplings involving hydroxyl groups were *ca.* 6-7 Hz, an indication of no particular preference for any orientation (data not shown). Thus, as previously stated[31] for **1** and its the deoxy analogues, HO-3 of disaccharides

TABLE V

^{19}F NMR chemical shifts (δ, ppm) and coupling constants (J, Hz) for compounds **2**, and **4-7** in D_2O solution at 37 °C.

Parameter	Compound				
	2	**4**	**5**	**6**	**7**
	δ_F, ppm				
	-234.0	-201.8	-219.7	-202.9	-233.1
	J, Hz				
$J_{F,C-3'}$	------	182.5	18.5	8.0	----
$J_{F,C-4,4'}$	6.2	17.4	178.0	179.4	7.9
$J_{F,C-6,6'}$	167.7	3.3	5.8	<1	165.5
$J_{F,C-1'}$	------	11.7	----	----	----
$J_{F,C-2'}$	------	18.4	<1	6.5	----
$J_{F,C-5,5'}$	17.5	7.6	17.6	14.7	20.0
$J_{F,H-3'}$	---	51.8	30.3	16.1	---
$J_{F,H-4'}$	---	6.5	50.3	50.9	---
$J_{F,H-6,6'}$	47.6	---	---	---	46.7
$J_{F,H-2'}$	---	14.0	---	---	---
$J_{F,H-5,5'}$	25.1	---	30.3	<1	14.8

TABLE VI

^1H NMR chemical shifts (δ,ppm) and chemical shift differences (Δδ) between 30 and 70 °C for the hydroxylic protons of **1-8** in DMSO-d_6.

Compound		Hydroxyl proton						
		OH-2	OH-3	OH-6	OH-2'	OH-3'	OH-4'	OH-6'
1	δ	5.12	4.63	4.53	5.04	4.73	4.46	4.61
	Δδ	0.27	0.08	0.21	0.21	0.26	0.21	0.18
2	δ	5.22	4.74	----	5.11	4.78	4.50	4.62
	Δδ	0.26	0.10	----	0.22	0.23	0.20	0.16
3	δ	5.22	4.70	----	5.17	4.70	4.49	4.62
	Δδ	0.27	0.09	----	0.20	0.25	0.22	0.19
4	δ	5.14	4.56	4.55	5.53	----	5.07	4.72
	Δδ	0.25	0.08	0.20	0.19	----	0.19	0.18
5	δ	5.13	4.49	4.57	5.32	5.32	----	4.90
	Δδ	0.25	0.08	0.20	0.20	0.21	----	0.18
6	δ	5.14	4.58	4.57	5.49	5.48	----	4.83
	Δδ	0.25	0.07	0.21	0.21	0.22	----	0.18
7	δ	5.17	4.50	4.56	5.18	4.96	4.78	----
	Δδ	0.25	0.08	0.20	0.18	0.21	0.20	----

TABLE VII

1H NMR vicinal coupling constants (J, Hz) for the lateral chains of the glucose and galactose residues of compounds **1-8** in D_2O and DMSO-d_6 solutions at 37 °C, and estimated populations of the different rotamers *gg*, *gt*, and *tg*.

$^3J_{H,H}$	Compound							
	1	**2**	**3**	**4**	**5**	**6**	**7**	**8**
Glucose residue								
D_2O								
$J_{5,6S}$	2.3	1.6	2.5	2.1	2.0	2.1	2.0	1.9
$J_{5,6R}$	5.2	2.5	6.1	5.0	---	5.0	5.0	4.8
%*gg*	60	95	50	65	60	60	60	65
%*gt*	40	5	50	35	40	40	40	35
DMSO-d_6								
$J_{5,6S}$	2.2	1.7	2.6	2.2	2.1	2.2	2.0	
$J_{5,6R}$	5.1	4.6	7.2	---	5.0	---	4.6	
%*gg*	60	75	40	60	60	60	65	
%*gt*	40	25	60	40	40	40	35	
Galactose residue								
D_2O								
$J_{5',6'S}$	4.0	---	---	---	5.4	---	3.5	6.0
$J_{5',6'R}$	8.2	---	---	---	6.9	---	7.6	7.0
%*tg*	20	---	---	---	40	---	20	35
%*gt*	70	---	---	---	50	---	65	60
%*gg*	10	---	---	---	10	---	15	5
DMSO-d_6								
$J_{5',6'S}$	4.0	---	---	---	6.3	---	3.7	
$J_{5',6'R}$	8.2	---	---	---	6.9	---	7.8	
%*tg*	20	---	---	---	45	---	20	
%*gt*	70	---	---	---	50	---	65	
%*gg*	10	---	---	---	5	---	15	

2-8 in methyl sulfoxide solution seems to be participating in interresidue hydrogen bonding, probably with O-5', as occurs in the crystal of β-lactose[32] and has been recently demonstrated in a detailed study[33] of methyl β-cellobioside in DMSO-d_6.

Hydroxymethyl conformation. Glucose and galactose $H6_{proR}$ and $H6_{proS}$ were assigned as previously reported for similar derivatives.[16,34] The distribution of rotamers was calculated for those compounds which showed resolved $J_{5,6}$ couplings (Table VII), following well established methodology[35] by using the Karplus-Altona[36] equation and assuming *gg:gt* and *gt:tg:gg* equilibria for the

glucose and galactose residues, respectively.[13, 16, 37] The observed couplings for the lateral chain of the different glucose residues can be explained for *ca.* 60:40 (±5) distributions of *gg* and *gt* rotamers. On the other hand, the values observed for the **D**-galactopyranose moieties agree with combinations of the *gt* and *tg* rotamers, being the *gt* family populated in extensions ≥65%. The observed couplings for compounds **2**, **6**, and **7** are very similar to those of their corresponding monosaccharides, as recently reported by Abraham and coworkers.[35] The main difference is observed for **2**, since our data indicate an almost exclusive participation of rotamer *gg*, while the data for methyl 6-deoxy-6-fluoro glucopyranoside indicate a participation of the *gt* rotamer. Therefore, the presence of the galactose moiety imposes a restriction through the C-5-C-6 bond of the glucose residue in compound **2** so that only the *gg* rotamer appears to exist in water. On the other hand, the presence of the glucose residue does not alter the distribution of rotamers around the C-5-C-6 bond of the galactose moiety, since the coupling constant values for **6** and **7** are almost identical to those reported for the corresponding methyl galactoside analogues. Vicinal $J_{F,H}$ agree with these observations, since $J_{F,H\text{-}5}$ of **2** is much larger than $J_{F,H\text{-}5'}$ of **7**, indicating an antiperiplanar disposition between the two coupled atoms in compound **2**. The distribution of rotamers is basically the same in both solvents, indicating that the polarity of water and methyl sulfoxide precludes the existence of the *tg* and *gg* rotamers for glucose and galactose, respectively. These rotamers could be stabilized by an intramolecular hydrogen bond between O-4 and O-6, as observed in molecular dynamics simulations in vacuo.[38]

Analysis of NOE data- An important handicap for the NOE-based conformational analysis of the lactose-type of disaccharides is the problem of severe overlap among H-3, H-4, and in some cases H-3', nuclei with potential or expected NOEs to H-1'. Nevertheless, the use of a specifically deuterated derivative of **1** showed[7,31] that the NOE to H-3 is practically nonexistent, fact corroborated indirectly with several deoxy analogues of **1**.[1,31] In the case of the halodeoxy derivatives presented in this study, H-4 does not overlap with H-3 in compounds **2**, **3**, and **8** in D_2O and in **2** and **3** in DMSO-d_6 solution. In addition, 2D-NOESY and 2D-ROESY experiments may alleviate the

TABLE VIII

Experimental 2D-CAMELSPIN (ROESY) cross peaks at mixing time 350 ms for compounds **2**, **3**, and **7** at 37 °C in D_2O and in DMSO-d_6 solution

Compound	Cross peak intensity (%)						
	H-1'/3'	H-1'/5'	H-1'/4	H-3'/4'	H-4'/5'	H-1/3	H-1/5
	D_2O 37°C						
3	4	4	5	5	5	4	5
	DMSO-d_6 37°C						
2	3	4	6	3	4	3	4
7	3	4	5	3	3	7[a]	7[a]

a. Overlapping signals

TABLE IX

Experimental and calculated steady-state NOEs for compounds **3**-**8** at 37 °C in D_2O solution upon saturation of H-1' resonance signal.

Compound	Observed NOE for signal(%)						
	H-2'	H-3'	H-4'	H-5'	H-4	H-6$_R$	H-6$_S$
3	5	10	-2	11	16	---	---
4	6	---	--	10	15	---	---
5	6	8	-1.5	9	18	0.5	0.5
6	8	8	--	11	19	1.0	1.0
7	5	10	--	11	19	0.5	0.5
8	5	9	-2	11	21	0.5	0.5
	Calculated NOE (%) for compound **1**[a]						
	H-2'	H-3'	H-4'	H-5'	H-4	H-6$_R$	H-6$_S$
Conformer A	7	9	-2	11	19	2	-0.5
Conformer B	5	8	-1	11	15	---	---
Conformer C	5	8	-2	11	18	---	---
Conformer C'	6	9	-2	11	22	---	---
Average	6	9	-2	11	18	0.5	---

a. Using the full matrix relaxation method and $\tau_c=0.09*10^{-9}$ s.
b. NOEs smaller than 1% are only approximated.

overlapping problem (Table VIII). In all these cases no H-1' to H-3 NOE was observed. In addition, for the other compounds, the problem may be resolved through the use of 2D-HSMQC-ROESY experiments which allow detection of NOEs using the carbon frequencies to remove the proton frequency degeneracy. A similar experiment, 2D-HMQC-NOESY has been recently used in the structural analysis of a biantennary oligosaccharide.[39] However, due to their correlation times, the smaller NOEs for disaccharides **1-8** prompted us to use rotating-frame NOEs to examine the possibility of H-1'-H-4 or H-1'-H-3 dipolar relaxation, but using the non-overlapping C-3 and C-4 ^{13}C NMR frequencies to label the cross-peak. An example of the experiment for compound **5** is given in Figure 4. The presence of cross-peaks H-1'/C-4, H-1'/C-5', and H-1'/C-3' can be noted, as well as the intraresidue H-1/C-3 and H-1/C-5 for the glucose ring. Therefore, it can be concluded that no important cross-relaxation between H-1' and H-3 does exist. Besides, the existence of NOE between H-1' and H-4 and not between H-2' and H-4 implies that compounds **1-8** spend most of its time in the region defined by local minima A, B, C, and C'. However, the differentiation among these geometries is rather difficult since their expected interresidue contacts are very similar. Nevertheless, the presence of NOE between H-1' and the H-6s protons indicate that the region defined by minimum A is populated to some extent. However, the fast equilibrium between the *gg* and *gt* rotamers with a different correlation time to that of the overall motion implies that the exact value of this NOE is very difficult to simulate. An estimation of interresidue distances may be obtained by use of the isolated spin pair approximation (ISPA), using the volumes of the cross peaks between proton pairs in NOESY or ROESY spectra acquired with a relatively short mixing time (Table VIII). This approximation leads to H-1'-H-4 distances in the range of 2.2-2.5 Å, as expected for the low energy area, but no discrimination among the different conformers is possible. The corresponding average distance for the studied compounds from MD simulations is 2.40 Å, although oscillations between 2.0 and 3.2 Å could be observed. The ISPA approximation produces average H-1'-H6s distances in between 3.0

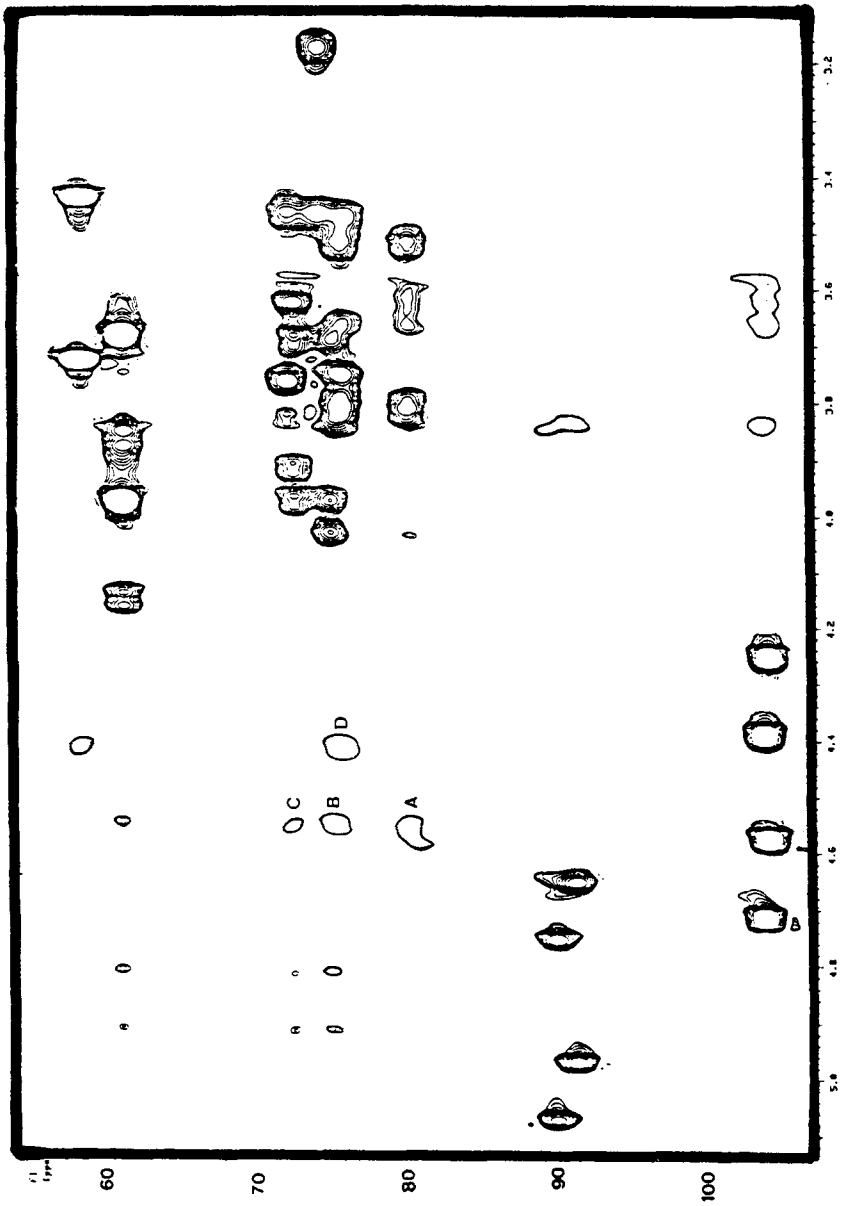

Figure 4.- HSMQC-ROESY spectrum (300 ms) at 37ºC of compound **5** in D_2O. Relevant cross-peaks are marked. (A) H-1'-C-4, (B) H-1'-C-5', (C) H-1'-C-3', (D) H-1-C-3/C-5. No cross-peaks between proton H-1' and carbon C-3 nor carbon C-5 can be observed.

TABLE X

Experimental and calculated NOESY intensities (mixing time=0.7 s) for compounds **3**, **4**, **7**, and **8** at 37 °C in D_2O solution.

Compound	Cross peak intensity (%)						
	H-1'/3'	H-1'/5'	H-1'/4	H-3'/4'	H-4'/5'	H-1/3	H-1/5
3	3	4	6	4	5	3	4
4	-	4	6	--	5	3	4
7	3	4	5	4	4	3	4
8	3	4	5	4	4	6[b]	6[b]
	Calculated intensity for compound **1**[a]						
	H-1'/3'	H-1'/5'	H-1'/4	H-3'/4'	H-4'/5'	H-1/3	H-1/5
Conformer A	3	4	6	4	4	3	4
Conformer B	3	4	5	4	4	3	4
Conformer C/C´	3	4	7	4	4	3	4
Average	3	4	6	4	4	3	4

a. Using $\tau_c=0.09*10^{-9}$ s. b. Overlapping signals.

and 3.5 Å, which also are compatible with the low energy region. Nevertheless, a more rigorous method to evaluate the experimental data is to use the geometries of the different minima to calculate the expected NOEs[20-22] *via* a complete relaxation matrix approach[20,26,27,29] using either one conformation or an average[30] according to a Boltzmann distribution function at a given temperature[40,41]. The results are collected in Tables IX-XII. The correlation times for compounds **2**, **3**, **5**, and **6** were estimated from ^{13}C NMR T_1 relaxation times in both solvents at two different temperatures (Table XIII). The observed average correlation times did not match the values of the intraresidue NOEs within the pyranoid rings which are conformation-independent and lead to smaller enhancements than those measured experimentally. A satisfactory match between the calculated and experimental intensities of H-1'-H-3', H-1'-H-5', and of H-1-H-3/H-5 in both steady state and 2D-NOESY experiments, was found by using average correlation times *ca.* 30-40% higher than those estimated from the ^{13}C-NMR relaxation measurements. A similar situation has been

TABLE XI

Experimental and calculated steady-state NOEs for compounds **2**, **3**, and **5** at 37 °C and 60 °C in DMSO-d_6 solution upon saturation of H-1' resonance signal.

	TEMP=37 °C						
Compound	Observed NOE for signal(%)						
	H-2'	H-3'	H-4'	H-5'	H-4	H-6_R	H-6_S
2	2	4	-0.3	5	8	---	---
3	2	3	-0.5	5	6	0.5	0.5
5	2	3	---	4	7	0.5	0.5
	Calculated NOE for compound **1**[a]						
	H-2'	H-3'	H-4'	H-5'	H-4	H-6_R	H-6_S
Conformer A	4	5	-0.3	5	8	0.5	---
Conformer B	3	4	-0.3	5	7	---	---
Conformer C	2	4	-0.3	5	7	---	---
Conformer C'	4	4	-0.3	5	10	---	---
Average	3	4	-0.3	5	8	0.2	---
	TEMP=60 °C						
Compound	Observed NOE for signal(%)						
	H-2'	H-3'	H-4'	H-5'	H-4	H-6R	H-6S
2	6	11	-0.5	11	16	---	---
3	6	8	-0.5	11	14	0.5	0.5
5	3	5	---	9	14	0.5	0.5
	Calculated NOE for compound **1**[b]						
	H-2'	H-3'	H-4'	H-5'	H-4	H-6R	H-6S
Conformer A	7	9	-1	10	16	2	----
Conformer B	5	8	-0.5	10	15	---	----
Conformer C	4	8	-0.5	10	16	---	----
Conformer C'	8	9	-1.0	10	20	---	----
Average	6	8	-1.0	10	17	0.5	----

a.$\tau_C=0.22*10^{-9}$ s.b.$\tau_C=0.12*10^{-9}$ s.c.NOEs smaller than 1% are only approximated.

previously described in different oligosaccharides.[42-44] The discrepancy could be due to the existence of anisotropic overall motion or to the presence of internal motions around the glycosidic linkages.[43] In fact, the observed relaxation times for C-4' were *ca.*

TABLE XII

Experimental and calculated NOESY intensities (mixing time=0.7 s) for compounds **2-4**, and **6** at 37 °C in DMSO-d6 solution.

Compound	Cross peak intensity (%)						
	H-1'/3'	H-1'/5'	H-1'/4	H-3'/4'	H-4'/5'	H-1/3	H-1/5
2	1	2	3	2	2	1	2
3	1	2	4	2	3	2	2
4	-	2	3	-	2	1	2
6	1	2	4	2	3	2	2
	Calculated intensity(%) for compound1[a]						
	H-1'/3'	H-1'/5'	H-1'/4	H-3'/4'	H-4'/5'	H-1/3	H-1/5
Conformer A	1	2	3	2	2	1	2
Conformer B	1	2	3	2	2	1	2
Conformer C	1	2	3	2	2	1	2
Conformer C'	1	2	4	2	2	1	2
Average	1	2	3	2	2	1	2

a. Using the full matrix relaxation method and $\tau_c=0.22*10^{-9}$ s.
b.c.d. Overlapping signals.

TABLE XIII

Experimental average methine ^{13}C NMR relaxation times (T_1, s) and corresponding average correlation times (τ_c, 10^{-9} s) for compounds **2**, **3**, **5**, and **6** in D_2O at 37 °C and DMSO-d_6 at 37 and 60 °C.

Compound	Solvent					
	D_2O		DMSO-d_6(37 °C)		DMSO-d_6(60 °C)	
	T_1	τ_c	T_1	τ_c	T_1	τ_c
2	0.74	0.07	0.43	0.13	0.61	0.09
3	0.70	0.08	0.43	0.13	0.62	0.09
5	0.73	0.07	0.37	0.15	0.62	0.09
6	0.72	0.07	0.37	0.15	0.63	0.09

15-20% smaller than those for the rest of the methine carbons, indicating a slight anisotropy of the overall motion. In addition, the relaxation times for C-6 and C-6' showed that the motion around both lateral chains is rather different, the one for the glucose moiety being more hindered.[13] The comparison among the observed

and calculated interresidue cross peaks H-1'-H-4 and H-1'-H-$6_{proS,R}$ for the different individual minima showed that a satisfactory match could be obtained by considering the presence of the different conformers A, B, C, and C' in the conformational equilibrium in both water and methyl sulfoxide since none of the individual geometries could fit all the NOE values simultaneously. The presence of conformers D or E in an appreciable extent (>5%) can be discarded since they would produce H-1'-H-4 intensities noticeably smaller than those measured along with observable NOE values for the H-1'-H-3 and/or H-2'-H-4 contacts that were never detected either in steady state or 2D-NOESY/ROESY measurements. These results indicate that the extent of flexibility around the β(1-4) linkage in halodeoxy lactosides **2-8** in water or methyl sulfoxide solutions is rather limited, since the NMR data can be satisfactorily explained by considering contributions of conformers defined by Φ=-100±40º and Ψ=-150±30º. Therefore, only *ca.* 5% of the complete potential energy surface is populated in solution. Therefore, the recognition of conformers in islands D or E should be accompanied by the formation of several hydrogen bonds or stabilizing van der Waals contacts to override the important energy barrier between the low energy area and these islands. According to our results, the glycosidic bonds of the halodeoxy derivatives of lactose **2-8** are not as flexible as observed for the β(1->4) linkage within the GM1 ganglioside[45] in methyl sulfoxide, but closer to the conclusions reached recently for the same glycosidic bond in the GM3 analogue,[27] the LeX trisaccharide,[26,29] 6'-*O*-sialyllactose,[13,46] and in a previous study of specifically deuterated **1**, based on ^{1}H NMR T_1 relaxation data,[47] although only conformation A was considered in the last report. The MD simulations produced average O-5'-O-3 distances of 2.95±0.10 Å indicating the possible presence of intramolecular hydrogen bond. Nevertheless, it has to be noted that this hydrogen bond does not seem to be essential to define the shape of these molecules. In fact, previous data for methyl 3-deoxy lactoside[1] and the LeX oligosaccharide have shown that their conformations are very similar to those reported in this paper. In fact, although the existence of the O-5'-O-3 hydrogen bond in methyl β-D-cellobioside has been recently demonstrated in DMSO-d_6, there are contradictory results in water since for methyl β-D-cellobioside it has been

proposed to disappear in water solution, at least for most of the time.[33] On the other hand, it has been postulated to exist in 6'-*O*-sialyl lactose.[46] In conclusion, compounds **1-8** show a very similar solution conformation, since all the experimental data can be described by a conformational equilibrium of the conformers included in the low energy region A-C′, as calculated from molecular mechanics and dynamics methods. Assuming that the interaction with the lectin takes place in one of these orientations,[7] the observed dissociation constants may be used to correlate structure and activity.

ACKNOWLEDGEMENTS

We thank Prof. M. Bernabé and Dr. A. Rivera (Madrid) for helpful discussions, Dr. M. Forster (Potters Bar, UK) for the use of the NOEMOL programme, Dr. A. Imberty (Nantes, France) for a preprint of reference 24 prior to publication, and Prof. M. Martín-Lomas for his continuous interest and support. Funding from DGICYT (grant PB-870367) is gratefully acknowledged.

REFERENCES

1. A. Rivera-Sagredo, D. Solis, T. Diaz-Mauriño, J. Jiménez-Barbero and M. Martín-Lomas, *Eur. J. Biochem.*,**197**, 217 (1991).

2. A. Rivera-Sagredo, D. Solis, T. Diaz-Mauriño, J. Jiménez-Barbero and M. Martín-Lomas, *Carbohydr. Res.*, **232**, 207 (1992).

3. R. U. Lemieux, L. T. J. Delbaere, H. Beierbeck and U. Spohr, *Ciba Foundation Symposium No. 158. Host Guest Molecular Interactions: from Chemistry to Biology* ,1990, Wiley.

4. C. P. J. Glaudemans, *Chem. Rev.*, **91**, 25 (1991).

5. P. S. Vermesch, J. J. G. Tesmer and F. A. Quiocho, *J. Mol. Biol.*, **226**, 923 (1992).

6. D. Solis, P. Fernandez, T. Diaz-Mauriño, J. Jiménez-Barbero and M. Martín-Lomas, *Eur. J. Biochem.*, **214**, 677, (1993).

7. V. L. Bevilacqua, D. S. Thomson and J. H. Prestegard, *Biochemistry,* **29**, 5529 (1990).

8. V. L. Bevilacqua, Y. Kim and J. H. Prestegard, *Biochemistry,* **31**, 9339 (1992).

9. R. Csuk and B. I. Glänzer, *Adv. Carbohydr. Chem. Biochem.*, **46**, 73 (1988).

10. C. Griesinger, G. Otting, K. Wüthrich and R. R. Ernst *J. Am. Chem. Soc.*, **110**, 7870 (1988).

11. (a)A. A. Bothner-By, R. L. Stephens, J.-M. Lee, C. D. Warren and R. W. Jeanloz, *J. Am. Chem. Soc.*, **106**, 811 (1984). (b) A. Bax and D. G. Davis, *J. Magn. Reson.*, **63**, 207 (1985).

12. H. Kessler, C. Griesinger, R. Kerssebaum, K. Wagner and R. R. Ernst, *J. Am. Chem. Soc.*, **109**, 607 (1987).

13. J. Breg, L. M. J. Kroon-Batenburg, G. Strecker, J. Montreuil and J. F. G. Vliegenthart, *Eur. J. Biochem.*, **178**, 727 (1989).

14. A. Bax and S. Subramanian, *J. Magn. Reson.*, **86**, 346 (1986).

15. E. R. P. Zuiderweg, *J. Magn. Reson.*, **67**, 565 (1990).

16. (a) Y. Nishida, H. Ohrui and H. Meguro, *Tetrahedron Lett.*, **25**, 1575 (1984). (b) H. Ohrui, Y. Nishida, M. Watanabe, H. Hori and H. Meguro, *Tetrahedron Lett.*, **26**, 3251 (1985) (c) D. M. Mackie, A. Maradufu and A. S. Perlin, *Carbohydr. Res.*, **150**, 23 (1986).

17. A. T. Hagler, S. Lifson and P. Dauber, *J. Am. Chem. Soc.*, **101**, 5122 (1979).

18. Discover 2.8 Program., *Biosym Technologies Inc.* San Diego, CA.

19. Insight 2.1.0 Program.,*Biosym Technologies Inc.* San Diego, CA.

20. (a) T. Peters, J.R. Brisson and D. R. Bundle, *Can. J. Chem.*, **68**, 979 (1990), and references therein. (b) B. R. Leeflang and L. M. J. Kroon-Batenburg, *J. Biomol. NMR*, **2**, 495 (1992).

21. (a) M. Forster, C. Jones and B. Mulloy, *J. Mol. Graph,* **7,** 196 (1989). (b) M. J. Forster, *J. Comput. Chem.* **12** 292 (1991).

22. D. Neuhaus and M. P. Williamson, *The Nuclear Overhauser Effect in Structural and Conformational Analysis* ; VCH Publishers, New York, 1989.

23. M. Bernabé, A. Fernández-Mayoralas, J. Jiménez-Barbero, M. Martín-Lomas and A. Rivera-Sagredo, *J. Chem. Soc. Perkin Trans. II,* 1867 (1989).

24. A. Imberty, Y. Bourne, C. Cambillau, P. Rouge and S. Perez, *Adv. Biophys. Chem.*, in press.

25. Y. Bourne, P. Rouge and C. Cambillau, *J. Biol. Chem.,* **267** , 197 (1992).

26. (a) S. W. Homans, *Biochemistry*, **29** , 9110 (1990). (b) S. W. Homans and M. Forster, *Glycobiology* , **2**, 143 (1992).

27. (a) H. C. Siebert, G. Reuter, R. Schauer, C. W. von der Lieth and J. Dabrowski, *Biochemistry* , **31**, 6962 (1992). (b) A. E. Aulabaugh, R. C. Crouch, G. E. Martin, A. Ragouzeos, J. P. Shockcor, T. D. Spitzer, R. D. Farrant, B. D. Hudson and J. C. Lindon, *Carbohydr. Res.,* **230**, 201 (1992).

28. K. Bock, *Pure Appl. Chem.*, **55**, 605 (1983).

29. K. E. Miller, C. Mukhopadhyay, P. Cagas and C. A. Bush, *Biochemistry,* **31**, 6703 (1992).

30. K. Bock, H. Lönn and T. Peters, *Carbohydr. Res.*,**198**, 375 (1990).

31. A. Rivera-Sagredo, J. Jiménez-Barbero and M. Martín-Lomas, *Carbohydr. Res.*, **221**, 37 (1991).

32. K. Hirotsu and A. Shimada, *Bull. Chem. Soc. Jpn.*, **47**, 1872 (1974).

33. B. R. Leeflang, J. F. G. Vliegenthart, L. M. J. Kroon-Batenburg, B. P. van Eijck and J. Kroon, *Carbohydr. Res.,* **230**, 41 (1992).

34. (a) Y. Nishida, H. Hori, H. Ohrui and H. Meguro, *J. Carbohydr. Chem.*, **7**, 239 (1988). (b) N. K. de Vries and H. M. Buck, *Carbohydr. Res.*, **165**, 1 (1987).

35. R. J. Abraham, E. J. Chambers and W. A. Thomas, *Carbohydr. Res.*, **226**, c1 (1992).

36. C. A. G. Haasnoot, F. A. A. M. de Leeuw and C. Altona, *Tetrahedron*, **36**, 2783 (1980).

37. K. Bock and S. Refn, *Acta Chem. Scand. B* , **41**, 469 (1987).

38. L. M. J. Kroon-Batenburg and J. Kroon, *Biopolymers*, **29**, 1243 (1990).

39. P. de Waard, B. R. Leeflang, J. F. G. Vliegenthart, R. Boelens, G. W. Vuister and R. Kaptein, *J. Biomol. NMR* , **2**, 211 (1992).

40. D. A. Cumming and J. P. Carver, *Biochemistry* , **26**, 6664 (1987).

41. A. Imberty, V. Tran and S. Perez, *J. Comput. Chem.*, **11**, 205 (1989).

42. P. Cagas and C. A. Bush, *Biopolymers*, **30**, 1123 (1990).

43. M. Hricovini, R. N. Shah and J. P. Carver, *Biochemistry*, **31**, 10018 (1992).

44. S. Sabesan, J. O. Duus, T. Fukunaga, K. Bock and S. Ludvigsen, *J. Am. Chem. Soc.*, **113**, 3236 (1991).

45. L. Poppe, C. W. von der Lieth and J. Dabrowski, *J. Am. Chem. Soc.*, **112**, 7762 (1990).

46. L. Poppe, R. Stuike-Prill, B. Meyer and H. van Halbeek, *J. Biomol. NMR* , **2**, 109 (1992).

47. P. C. Kline, A. S. Serianni, S. G. Huang, M. Hayes and R. Baker, *Can. J. Chem.*, **68**, 2171 (1990).